Supporting Information:

DNA-Cholesterol Barges as Programmable

Membrane-Exploring Agents

Alexander Johnson-Buck[1], Shuoxing Jiang[2,3], Hao Yan[2,3], and Nils G. Walter[1]*

[1]Single Molecule Analysis Group, Department of Chemistry, 930 N. University Ave., University of

Michigan, Ann Arbor, MI 48109-1055, USA

[2]The Biodesign Institute, Arizona State University, Tempe, Arizona 85287, USA

[3]Department of Chemistry and Biochemistry, Arizona State University, Tempe, Arizona 85287,

USA

*nwalter@umich.edu

Table of Contents

Linker Strand	Sequence
1	5'-CAACATGTATTGCTGAATATAATGACCAGTAA
2	5'-CCCCCTCAAATCGTCATAAATATTAATCAATA
3	5'-AATCTACGACCAGTCAGGACGTTGTTCATCAA
4	5'-GAACCGAAAGGCGCAGACGGTCAAATTAATTA
5	5'-CGGAACGAACCCTCAGCAGCGAAACGCGAGAA
6	5'-ACAGTTTCTGGGATTTTGCTAAACCGACAAAA
7	5'-GGTAAAGTAGAGAATATAAAGTACAACTTTCA
8	5'-AACTTTTTATCGCAAGACAAAGAAGACAGCAT
9	5'-CATTTAACACATCAAGAAAACAAATCATAAGG
10	5'-TATAATCCTATCAGATGATGGCAAGGAAGAAA
11	5'-TCTGGTCACAAATATCAAACCCTCCATTGAAT
12	5'-TAAAAGGGATTCACCAGTCACACGCTGTAGCT

Table S1. Sequences of linker strands used to induce DNA barge oligomerization as described in Li, Z.; Liu, M.; Wang, L.; Nangreave, J.; Yan, H.; Liu, Y. *J. Am. Chem. Soc.* **2010**, *132*, 13545–13552.
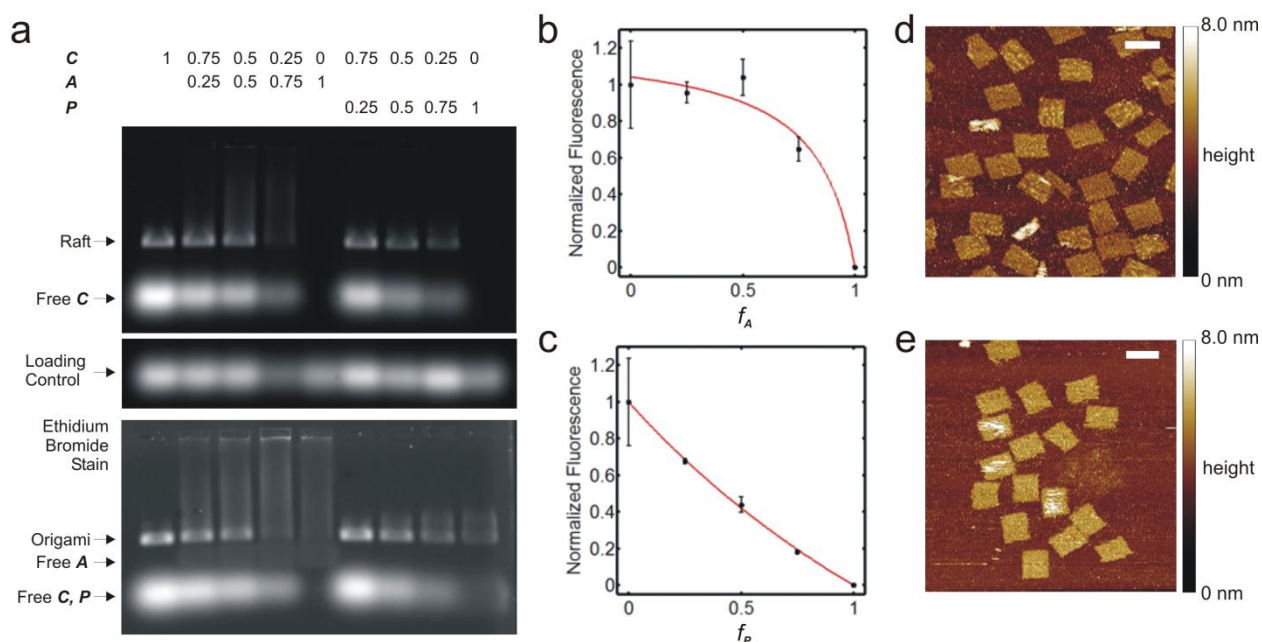

Figure S1. Assembly and aggregation of DNA barges. (a) 0.5% agarose gel showing Cy3 fluorescence and aggregation of DNA barges as a function of the mole fractions of *A*, *C*, and *P* used in assembly. Results from ethidium bromide staining are also shown in the lower panel; note that some crosstalk from Cy3 is observed in the ethidium scan. (b,c) Fluorescence of Cy3-labeled *C* bound to DNA barges as a function of the mole fraction of *A* (b) or *P* (c). The plots in (b) and (c) are evaluated by fitting with equation (1) (see Materials and Methods) to extract the relative rate constants of *A*, *C*, and *P* binding to DNA barges (k_A, k_C, and k_P). Based on these fits, $k_A/k_C = 0.153$ and $k_P/k_C = 1.36$. Error bars represent the standard error of the mean from three separate replicates. (d, e) Atomic force micrographs of DNA origami before (d) and after (e) addition of a 1:1 mixture of *A* and *P* oligonucleotides. Scale bars: 100 nm.
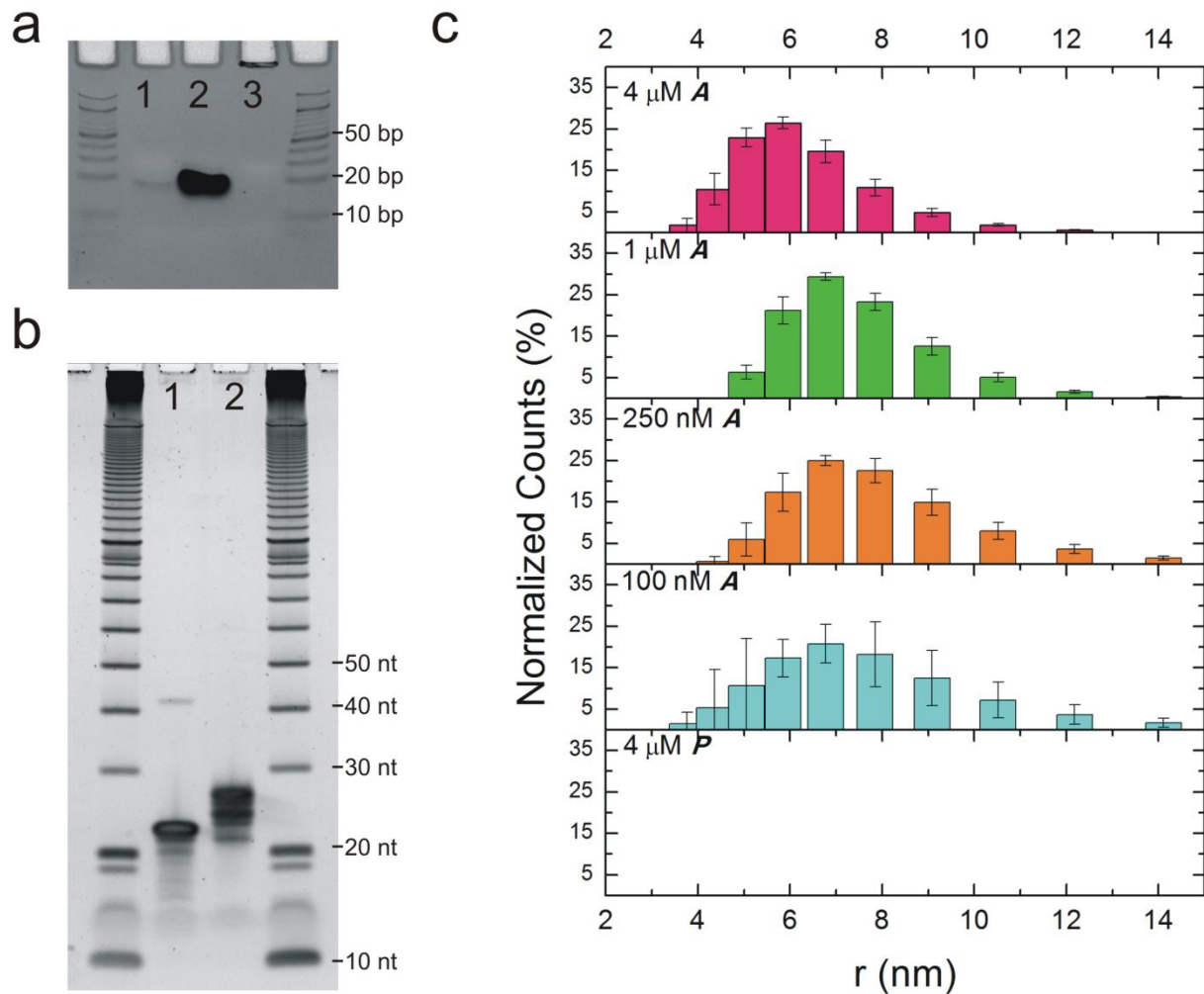
Figure S2. Aggregation of cholesterol-labeled **A** in aqueous solution. (a) Non-denaturing PAGE characterization of **A**, **C'**, and **P** oligonucleotides. Lane 1: **P**; Lane 2: **C'**; Lane 3: **A**. The retention of **A** in the sample well is consistent with cholesterol-induced aggregation into micelles. The main band for **C'** appears darker than for the other samples due to signal contamination from Cy3 fluorescence. (b) Denaturing PAGE characterization of **A** and **P**. Lane 1: **P**; Lane 2: **A**. (c) DLS characterization of the aggregation of **A** into micelles in aqueous solution, together with **P** as a negative control. Error bars correspond to one standard deviation from three independent trials.
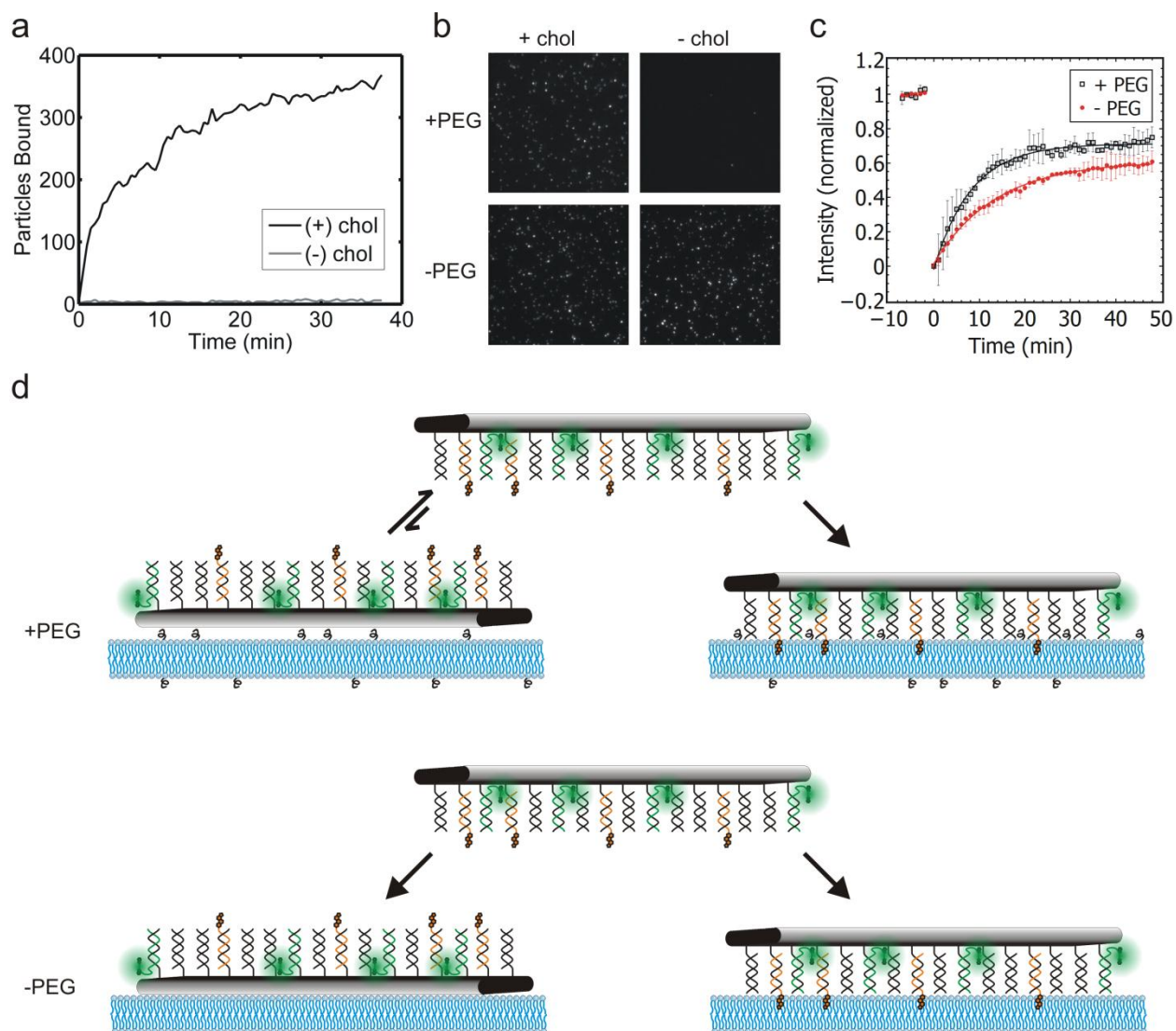
Figure S3. Kinetics and extent of DNA barge binding to supported lipid bilayers. (a) Kinetics of binding to a DOPC-DOPE/mPEG bilayer. (b) Representative portions of fields of view showing the density of DNA barges bound to bilayers with or without DOPE-mPEG after binding had reached completion. DNA barges were prepared using **A**:**C**:**P** ratios of either 1:1:2 ('(+) chol') or 0:1:3 ('(-) chol'). (c) Fluorescence recovery after photobleaching (FRAP) measurements for supported lipid bilayers containing either DOPC ('- PEG') or DOPC + DOPE-mPEG ('+ PEG'). Error bars are standard deviations from two replicates performed on separate slides on different days. The recovery curves are fit with the single-exponential function $y = A*\exp(-t/\tau) + y_0$; parameters derived from fitting are τ = 8.2 min, y_0 = 0.71 (+ PEG) and τ = 13.6 min, y_0 = 0.61 (- PEG). (d) Model of the effect of PEGylated lipid head groups upon specific vs. nonspecific binding of DNA origami to supported lipid bilayers.
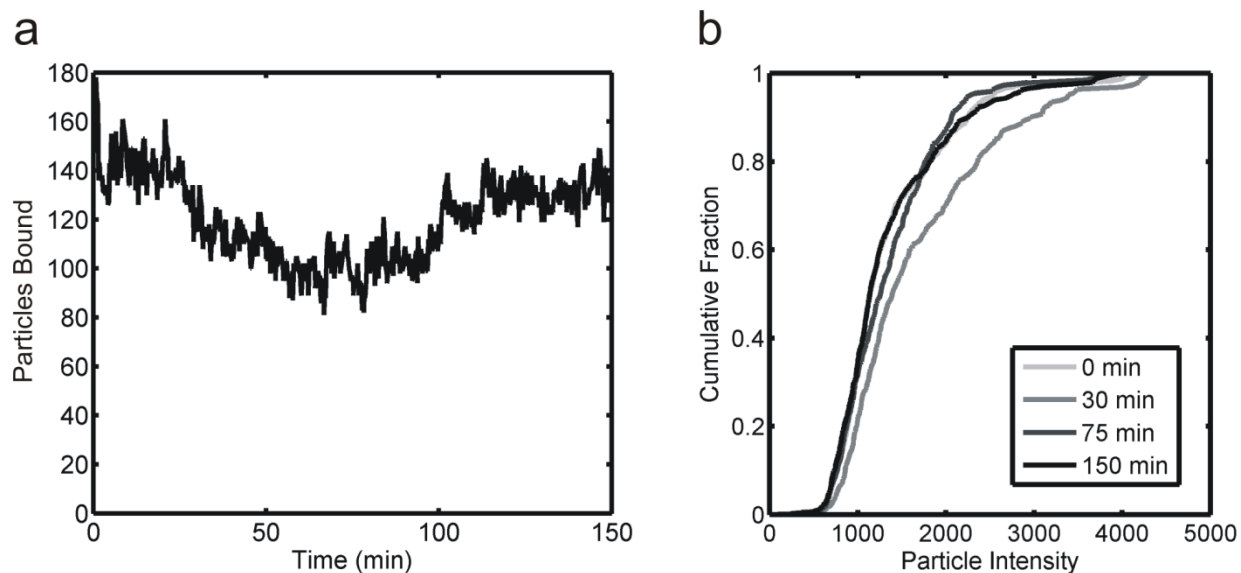
Figure S4. Control for dissociation and aggregation of DNA barges associated with a DOPC/DOPE-mPEG bilayer in absence of fuel or polymerization strands as observed by TIRF microscopy. (a) Number of barges observed as a function of time in a single field of view. (b) Cumulative intensity distribution of barges in the same field of view as (a) over time. A blank solution containing buffer and oxygen scavenger was introduced after 2 min. In contrast to lift-off (Fig. 4b, main text) or polymerization (Fig. 5, main text) experiments, there is no evidence of significant dissociation from the membrane or aggregation of DNA barges when the appropriate command oligonucleotides are omitted.
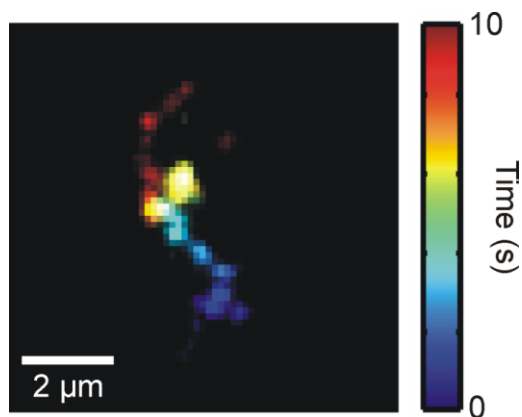

Figure S5. Time-lapse image showing the lateral diffusion of a DNA barge assembled with a 0:1:3 mixture of *A:C:P* (i.e., lacking cholesterol anchors) associated with a DOPC/DOPE-mPEG bilayer. Each frame from the raw movie is shown in a different color as indicated by the scale bar on the right.
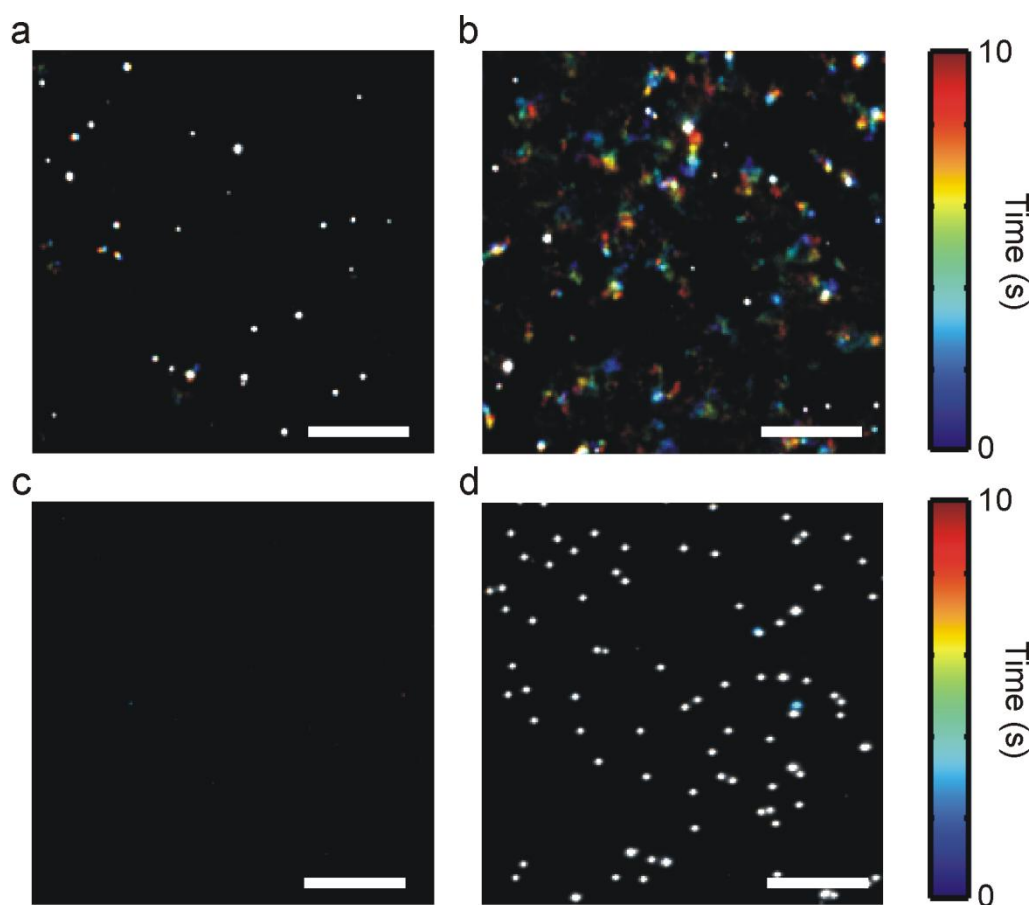
S6

Figure S6. Time-lapse images of DNA barge binding to supported lipid bilayers containing DOPC or to a bare glass surface. (a) DOPC bilayer after incubation with DNA barges lacking cholesterol anchors (0:1:3 ratio of *A*:*C*:*P*) in the presence of TA-Mg^{2+}. Nearly all observed barges are immobile on the timescale of observation. (b) DOPC bilayer after incubation with DNA barges bearing cholesterol anchors (1:1:2 ratio of *A*:*C*:*P*) in the presence of TA-Mg^{2+}. The majority of barges are diffusing laterally. (c) DOPC bilayer after incubation with DNA barges lacking cholesterol anchors (0:1:3 ratio of *A*:*C*:*P*) in the presence of PBS (no barges are visible). (d) Bare glass slide after incubation with DNA barges (1:1:0 ratio of *A*:*C*:*P*) in the presence of PBS. No lateral diffusion is observed. Scale bars: 10 μm.
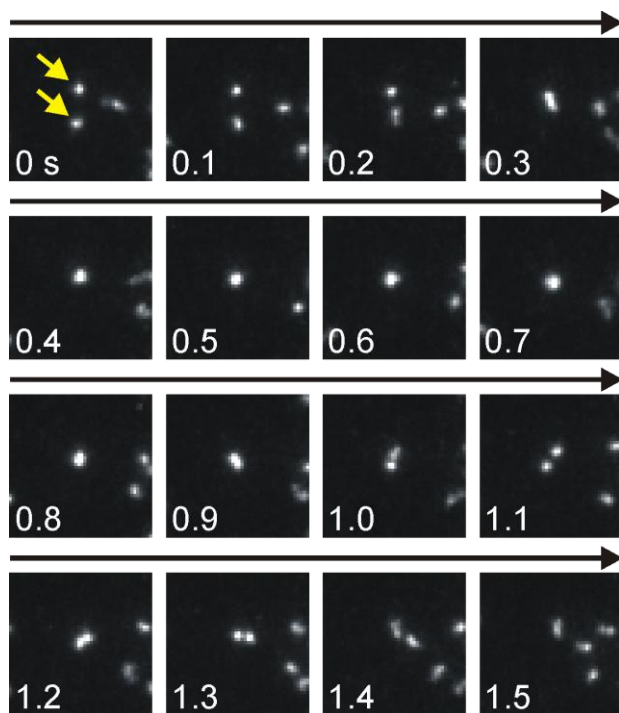
Figure S7. Example of apparent transient interaction between two DNA barges, indicated by the yellow arrows, within a DOPC/DOPE-mPEG bilayer. The two barges occupy approximately the same diffraction-limited region for ~0.5 s.
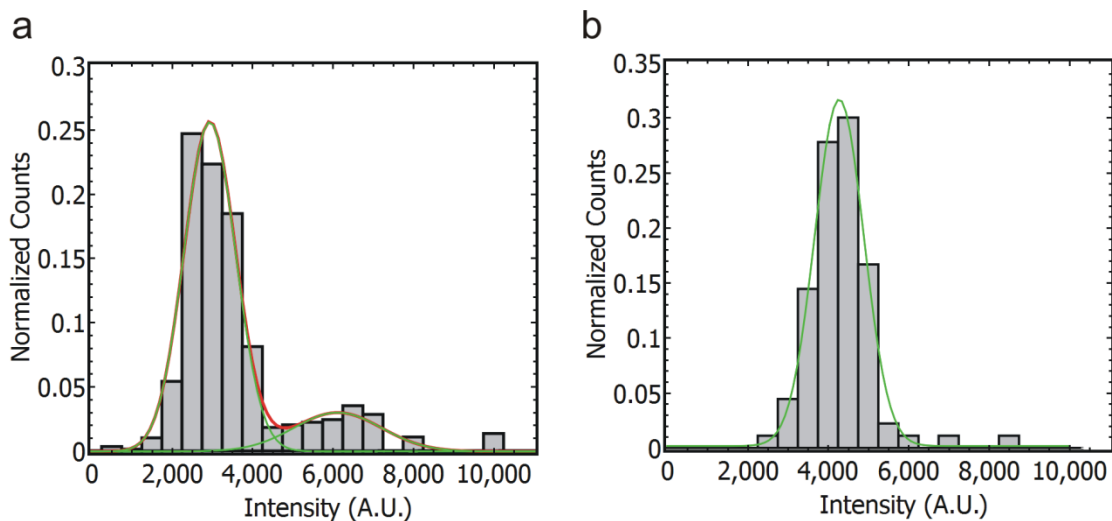

Figure S8. (a) Intensity histogram derived from 242 DNA barges (or unresolved complexes) associated with a DOPC/DOPE-mPEG bilayer in TA-Mg^{2+}, along with two best-fit Gaussian functions centered on intensity values of ~2,940 (84%) and ~6,120 (16%). Barges were assembled with a 1:1:2 mixture of *A*:*C*:*P*. (b) Intensity histogram derived from 90 DNA barges associated with a DOPC bilayer in PBS within a single field of view, along with a best-fit Gaussian function centered on intensity value ~4,278. Barges were assembled with a 1:1:0 mixture of *A*:*C*:*P*.
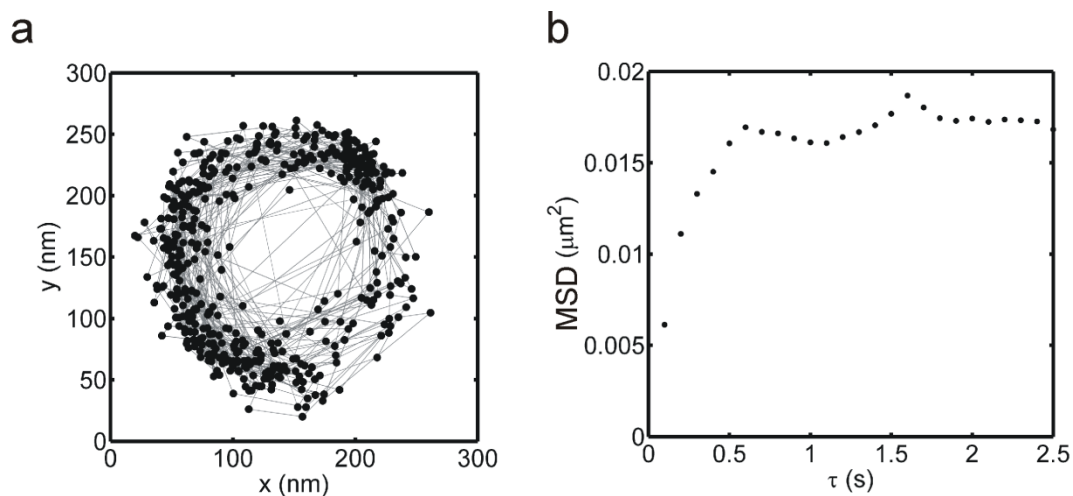
Figure S9. Apparent diffusion of a DNA barge about an isolated lipid vesicle. (a,b) Trajectory (a) and mean squared displacement (MSD) (b) of a single DNA barge (*A:C:P* = 1:1:0, in PBS) undergoing corralled diffusion within a small region on a slide coated with a patchy DOPC bilayer. The behavior is suggestive of confinement of the DNA barge on a vesicle 150-200 nm in diameter. The duration of the trajectory shown in (a) is 50 s.
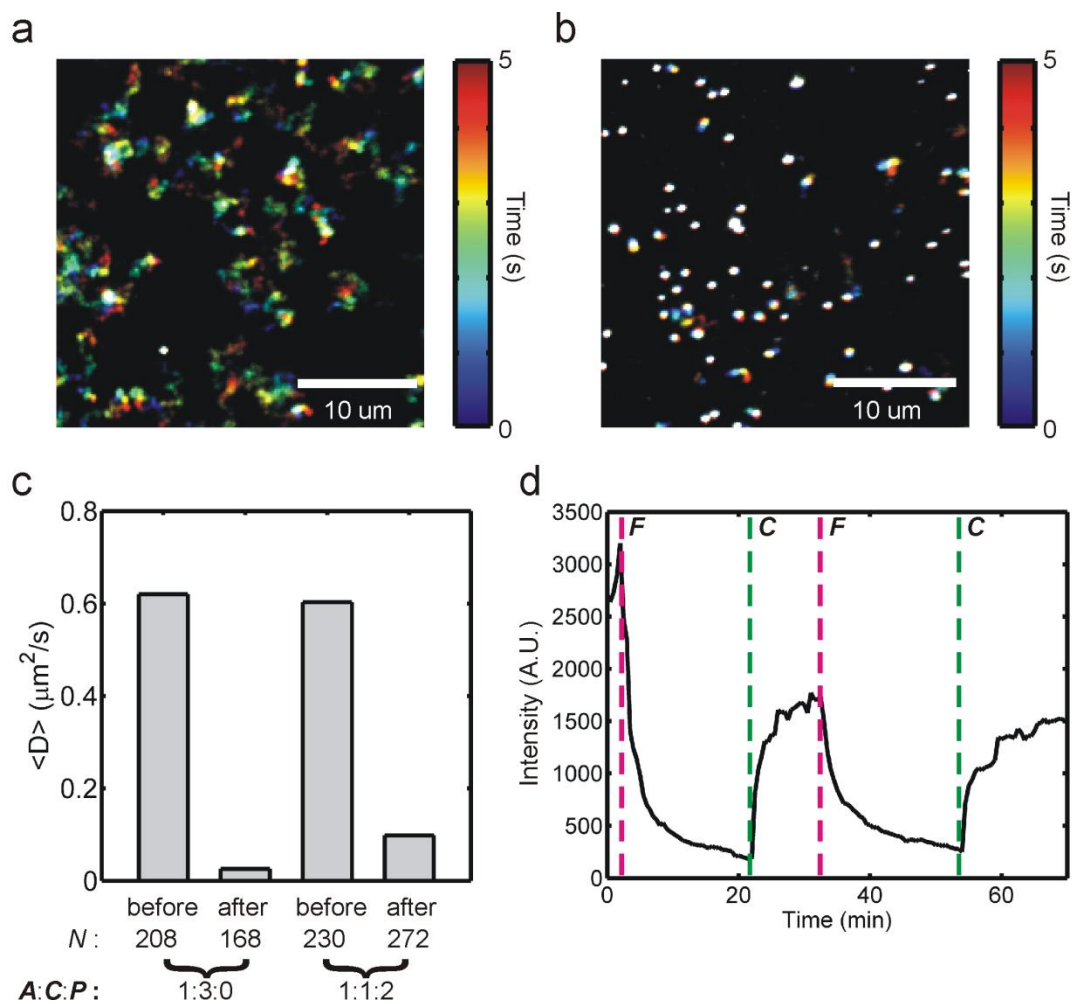
Figure S10. Slowing of diffusion and incomplete reloading upon displacement of Cargo from DNA barges. (a,b) Time-lapse images of DNA barges prepared with a 1:3:0 ratio of **A:C:P** before (a) and after (b) two cycles (removal and addition) of Cargo exchange, showing the marked decrease in the rate of lateral diffusion. The decrease in rate of diffusion is noticeable during the first unloading of Cargo. (c) Mean diffusion coefficients of DNA barges of different **A:C:P** compositions before and after two consecutive cycles (removal and addition) of Cargo exchange. *N* barge trajectories within a single field of view were used in each determination of *<D>*. (d) Incomplete recovery of fluorescence intensity after adding fuel (**F**) and fresh Cargo (**C**) to membrane-associated 1:3:0 **A:C:P** barges.